Available online at www.sciencedirect.com
SCIENCE DIRECT®
Wave Motion 41 (2005) 247–261
WAVE MOTION
www.elsevier.com/locate/wavemoti

Transient elastic waves applied to nondestructive testing of transversely isotropic lossless materials: a coordinate-free approach

Karl J. Langenberg, René Marklein*

University of Kassel, Department of Electrical Engineering and Computer Science, Electromagnetic Theory, D-34109 Kassel, Germany

Received 5 December 2003; received in revised form 3 May 2004; accepted 10 May 2004
Available online 27 September 2004

Abstract

Transient plane wave theory for anisotropic, in particular transversely isotropic lossless materials is formulated and evaluated as a coordinate-free approach leading to comparatively simple analytical expressions for phase wave speeds, polarization vectors and energy wave speeds. The application to the practical problem of nondestructive testing of dissimilar welds yields a concise physical interpretation of the output of numerical simulation codes.

Keywords: Elastic wave propagation; Nondestructive testing; Transversely isotropic lossless materials; Numerical modeling; Elastodynamic finite integration technique (EFIT); Plane wave propagation; Phase wave velocity, polarization vector and energy wave velocity

1. Introduction

In general, primary circuit pipe welds of nuclear power plants are so-called dissimilar welds consisting of austenitic steel embedded in ferritic steel. Fig. 1 shows a typical polished cut of such a weld: Due to the welding process a granular structure is created, which makes the weld an anisotropic medium for elastic waves; typically, the weld is often buffered to the isotropic ferritic pipe material by a layer of austenitic steel exhibiting a horizontal grain orientation, and an austenitic cladding of the interior of the pipe with a vertical grain orientation makes the embedding of the weld even more “dissimilar”.

Therefore, the detection of cracks growing from the interior pipe wall into the weld region through the excitation of impulsive elastic waves in the ultrasonic frequency regime (∼2 MHz) from the exterior pipe wall definitely requires

* Corresponding author. Tel.: +49 561 804 6426; fax: +49 561 804 6489.
E-mail addresses: langenberg@uni-kassel.de (K.J. Langenberg); marklein@uni-kassel.de (R. Marklein).

0165-2125/$ – see front matter © 2004 Elsevier B.V. All rights reserved.
doi:10.1016/j.wavemoti.2004.05.007

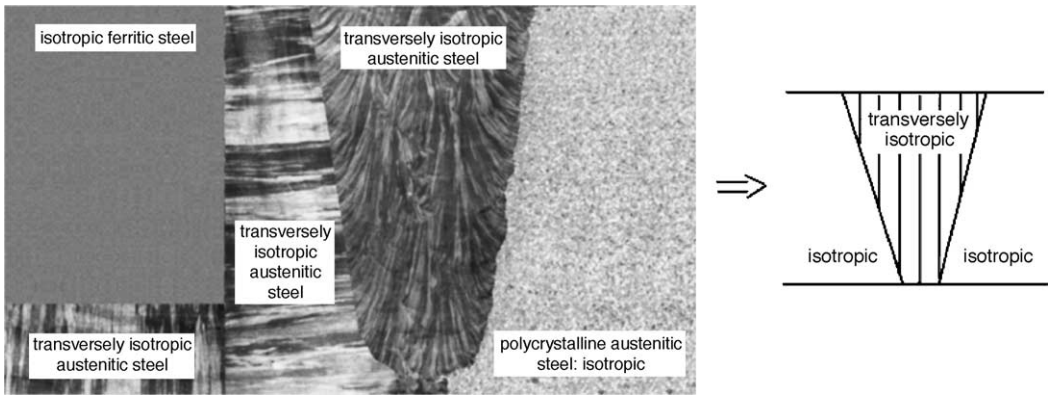

Fig. 1. Polished cut of a dissimilar weld (left) and zero-order computer model for elastic wave propagation (right: vertical homogeneous grain orientation).

the interpretation of recorded transient signals of considerable complexity. Of course, elastic wave propagation *modeling* can help to understand the physical contents of such signals. Unfortunately, even for the zero-order computer model of an austenitic weld as it is displayed in Fig. 1—homogeneous weld material with transverse isotropy embedded in a homogeneous isotropic material—the required Green functions (tensors) to formulate transducer aperture radiation as well as scattering analytically [1] are only available as rather complicated integral representations [2]. On the other hand, numerical methods operating directly on the underlying elastodynamic governing equations serve as an excellent modeling tool not only to predict transient recorded signals but to reveal all physical aspects of elastic wave radiation, propagation and scattering: The optically opaque weld is made transparent. Fig. 2 gives an example as it is obtained with the two-dimensional version of the Elastodynamic Finite Integration Technique (EFIT: [3–8]) for the zero-order geometry of Fig. 1. If the same geometry, yet under the assumption of an *isotropic* weld material—polycrystalline austenitic steel with approximately the same material as ferritic steel—is similarly investigated (see Fig. 3), the mere optical comparison of the time snap shots of both figures reveals the "strange" refraction effects at the surface separating the anisotropic (transversely isotropic) weld from the isotropic ferritic embedding material; a potential crack growing from the interior pipe wall along the right boundary of the weld would not be hit by the refracted wave front as it would be true for an isotropic weld material. Hence, modeling is mandatory to design an ultrasonic experiment correctly, but the question is whether one has to rely on complicated analytical and/or extensive numerical modeling or if simpler tools are at hand for an initial guess of what would happen in an environment as displayed in Fig. 1. As a matter of fact, comparatively simple plane wave theory can help to predict the output of an ultrasonic experiment if the focus is on transient plane wave energy rays. It turns out that explicit analytical formulas for energy wave speeds and directions in transversely isotropic materials are immediately at hand (and simpler than those previously published: [9]) if one disregards the definition of a group velocity in favor of the energy velocity, and, in particular, if one concentrates on a coordinate-free approach (consequently applied to electromagnetic waves by Chen [10]) instead of the conventional indicial notation together with the summation convention [1,11–13]. The latter has the disadvantage that equations, in particular if they contain the Levi-Cività ϵ_{ijk}-tensor, must be read very carefully, whereas a coordinate-free notation leads to a perfectly clear and immediately visible mathematical representation of the underlying physics. Yet the most convincing argument for a coordinate-free calculus is the straightforward computation of determinants, adjoints and inverses of tensors as provided by H.C. Chen [10] (compare Section 2.3). Of course, if it comes to numerical calculations, the introduction of coordinates cannot be avoided.

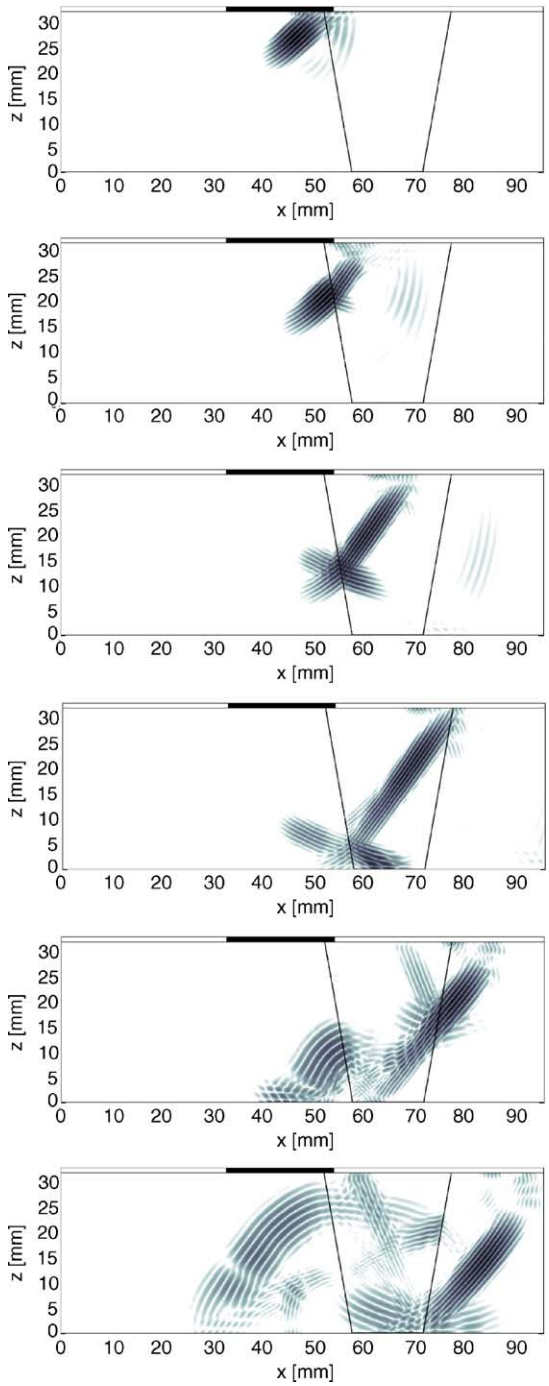

Fig. 2. 2D-EFIT modeling: radiation, propagation and scattering of a 45°-shear-vertical elastic wave: austenitic weld material is assumed to be transversely isotropic with the lines in Fig. 1 indicating the granular preference direction; the bar on top of the exterior pipe wall indicates the size and the location of the exciting aperture (ferritic steel: pressure wave speed 5900 m/s, shear wave speed 3200 m/s, mass density 7700 kg/m^3; for Lamé constants of transversely isotropic austenitic steel compare Fig. 4).

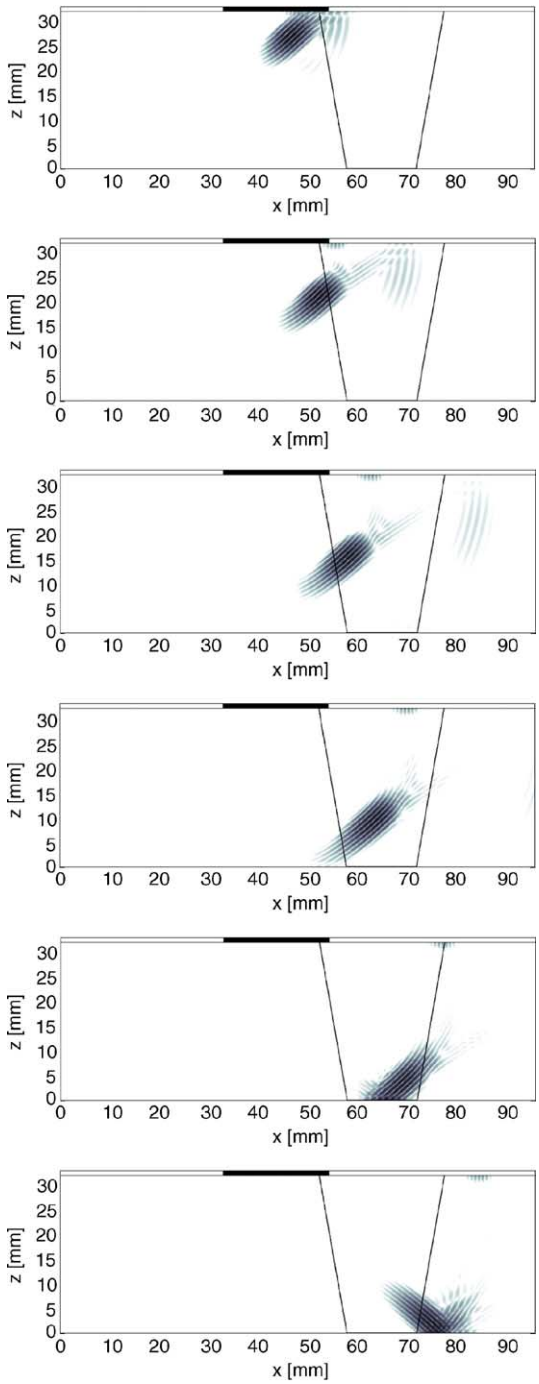

Fig. 3. 2D-EFIT modeling: radiation, propagation and scattering of a 45°-shear-vertical elastic wave: austenitic weld material is assumed to be polycrystalline isotropic; the bar on top of the exterior pipe wall indicates the size and the location of the exciting aperture (polycrystalline austenitic steel: pressure wave speed 5600 m/s, shear wave speed 3100 m/s, mass density 7900 kg/m^3).

2. Elastic plane waves in transversely isotropic lossless materials

2.1. Governing and constitutive equations; wave equation

The governing equations of linear elastodynamics—Newton-Cauchy equation of motion, deformation rate equation—for the field quantities $\underline{\mathbf{j}}(\underline{\mathbf{R}}, t)$ (momentum density vector), $\underline{\underline{\mathbf{T}}}(\underline{\mathbf{R}}, t)$ (second rank stress tensor), $\underline{\underline{\mathbf{S}}}(\underline{\mathbf{R}}, t)$ (second rank strain tensor), $\underline{\mathbf{v}}(\underline{\mathbf{R}}, t)$ (particle velocity vector) and the sources $\underline{\mathbf{f}}(\underline{\mathbf{R}}, t)$ (volume force density vector) and $\underline{\underline{\mathbf{h}}}(\underline{\mathbf{R}}, t)$ (second rank injected deformation rate tensor)—$\underline{\mathbf{R}}$ is the vector of position and t the time—read[1] (for a precise and consistent derivation see [1])

$$\frac{\partial \underline{\mathbf{j}}(\underline{\mathbf{R}}, t)}{\partial t} = \nabla \cdot \underline{\underline{\mathbf{T}}}(\underline{\mathbf{R}}, t) + \underline{\mathbf{f}}(\underline{\mathbf{R}}, t), \tag{1}$$

$$\frac{\partial \underline{\underline{\mathbf{S}}}(\underline{\mathbf{R}}, t)}{\partial t} = \underline{\underline{\underline{\mathbf{I}}}}^{+} : \nabla \underline{\mathbf{v}}(\underline{\mathbf{R}}, t) + \underline{\underline{\mathbf{h}}}(\underline{\mathbf{R}}, t), \tag{2}$$

each dot stands for the contraction of adjacent indices of the respective vectors (one underline) and (second rank) tensors (two underlines); the forth rank tensor $\underline{\underline{\underline{\mathbf{I}}}}^{+}$ yields the symmetric part of a second rank tensor (in this case the gradient dyadic of the particle velocity vector) under double contraction. These governing equations *must* be complemented by constitutive equations relating the field quantities; these read for linear time-invariant instantaneously and locally reacting homogeneous anisotropic materials [1]:

$$\underline{\mathbf{j}}(\underline{\mathbf{R}}, t) = \rho \underline{\mathbf{v}}(\underline{\mathbf{R}}, t), \tag{3}$$

$$\underline{\underline{\mathbf{T}}}(\underline{\mathbf{R}}, t) = \underline{\underline{\underline{\mathbf{c}}}} : \underline{\underline{\mathbf{S}}}(\underline{\mathbf{R}}, t), \tag{4}$$

thus defining the scalar mass density ρ and the forth rank stiffness tensor $\underline{\underline{\underline{\mathbf{c}}}}$, which, due to the symmetry of $\underline{\underline{\mathbf{S}}}$ (by definition) and $\underline{\underline{\mathbf{T}}}$ (by conservation of angular momentum) together with conservation of energy obeys the symmetries $\underline{\underline{\underline{\mathbf{c}}}}^{1234} = \underline{\underline{\underline{\mathbf{c}}}}^{2134} = \underline{\underline{\underline{\mathbf{c}}}}^{1243} = \underline{\underline{\underline{\mathbf{c}}}}^{3412}$, where the upper indicial notation accounts for the permutational replacement of tensor elements. With these constitutive equations we readily arrive at the wave equation

$$\nabla \cdot \underline{\underline{\underline{\mathbf{c}}}} : \nabla \underline{\mathbf{v}}(\underline{\mathbf{R}}, t) - \rho \frac{\partial^2 \underline{\mathbf{v}}(\underline{\mathbf{R}}, t)}{\partial t^2} = -\frac{\underline{\mathbf{f}}(\underline{\mathbf{R}}, t)}{\partial t} - \nabla \cdot \underline{\underline{\underline{\mathbf{c}}}} : \underline{\underline{\mathbf{h}}}(\underline{\mathbf{R}}, t), \tag{5}$$

which turns into a homogeneous time-harmonic reduced wave equation for the Fourier-transformed particle displacement

$$\nabla \cdot \underline{\underline{\underline{\mathbf{c}}}} : \nabla \underline{\mathbf{u}}(\underline{\mathbf{R}}, \omega) + \rho \omega^2 \underline{\mathbf{u}}(\underline{\mathbf{R}}, \omega) = \underline{\mathbf{0}}, \tag{6}$$

if we put sources equal to zero and define

$$\underline{\mathbf{v}}(\underline{\mathbf{R}}, \omega) = \int_{-\infty}^{\infty} \underline{\mathbf{v}}(\underline{\mathbf{R}}, t) \mathrm{e}^{\mathrm{j}\omega t} \mathrm{d}\omega = -\mathrm{j}\omega \underline{\mathbf{u}}(\underline{\mathbf{R}}, \omega), \tag{7}$$

$\mathrm{j} = \sqrt{-1}$ being the imaginary unit.

[1] Note: Considering both kinds of sources is very helpful for the derivation and interpretation of an elastodynamic Huygens-type representation and extinction theorem [14].

2.2. Phase and energy wave speeds of time-harmonic plane waves in lossless anisotropic materials

2.2.1. Homogeneous plane waves

In the time-harmonic plane wave ansatz—$u(\omega)$ representing the Fourier-spectrum of the arbitrary (causal) time domain impulse $u(t)$—

$$\underline{\mathbf{u}}(\underline{\mathbf{R}},\omega) \Longrightarrow \underline{\mathbf{u}}(\underline{\mathbf{R}},\omega,\hat{\underline{\mathbf{k}}}) = u(\omega)\hat{\underline{\mathbf{u}}}(\hat{\underline{\mathbf{k}}})\mathrm{e}^{\mathrm{j}(\hat{\underline{\mathbf{k}}}\cdot\underline{\mathbf{R}}/c(\hat{\underline{\mathbf{k}}}))\omega}, \tag{8}$$

involving the prescribed unit-vector $\hat{\underline{\mathbf{k}}}$ of the phase propagation direction—planes of constant phase are orthogonal to $\hat{\underline{\mathbf{k}}}$—we have to determine the phase speed $c(\hat{\underline{\mathbf{k}}})$ and the polarization unit-vectors $\hat{\underline{\mathbf{u}}}(\hat{\underline{\mathbf{k}}})$. They come as solutions of the eigenvalue problem

$$\underline{\underline{\mathbf{D}}}(\hat{\underline{\mathbf{k}}})\cdot\hat{\underline{\mathbf{u}}}(\hat{\underline{\mathbf{k}}}) = c^2(\hat{\underline{\mathbf{k}}})\hat{\underline{\mathbf{u}}}(\hat{\underline{\mathbf{k}}}), \tag{9}$$

for the real-symmetric positive-definite Kelvin–Christoffel tensor

$$\underline{\underline{\mathbf{D}}}(\hat{\underline{\mathbf{k}}}) = \frac{1}{\rho}\hat{\underline{\mathbf{k}}}\cdot\underline{\underline{\underline{\mathbf{c}}}}\cdot\hat{\underline{\mathbf{k}}}, \tag{10}$$

where the square of the phase speed appears as eigenvalue. Anisotropic materials are characterized by a direction dependence of the phase speed, and, moreover, by a direction dependence of the energy wave speed together with the non-coincidence of phase and energy propagation directions. Note: It is much more intuitive to use the energy wave speed instead of the group velocity, because the latter one can only be defined approximately for wave packets under certain assumptions whereas the first one makes always sense; in particular, explicit expressions for the energy speed are available for transversely isotropic materials which are considerably simpler than those for the group velocity [9].

The energy wave speed is defined through

$$\underline{\mathbf{c}}_{\mathrm{E}}(\hat{\underline{\mathbf{k}}}) = \frac{\Re\underline{\mathbf{S}}_{\mathrm{K}}(\underline{\mathbf{R}},\omega,\hat{\underline{\mathbf{k}}})}{\langle w_{\mathrm{el}}(\underline{\mathbf{R}},t,\hat{\underline{\mathbf{k}}})\rangle}, \tag{11}$$

where $\underline{\mathbf{S}}_{\mathrm{K}}$ is the complex elastodynamic Poynting-vector and $\langle w_{\mathrm{el}}(\underline{\mathbf{R}},t,\hat{\underline{\mathbf{k}}})\rangle$ the time averaged elastodynamic energy density of time harmonic plane waves:

$$\underline{\mathbf{S}}_{\mathrm{K}}(\underline{\mathbf{R}},\omega,\hat{\underline{\mathbf{k}}}) = \tfrac{1}{2}\mathrm{j}\omega\,\underline{\mathbf{u}}(\underline{\mathbf{R}},\omega,\hat{\underline{\mathbf{k}}})\cdot\underline{\underline{\mathbf{T}}}^{*}(\underline{\mathbf{R}},\omega,\hat{\underline{\mathbf{k}}}), \tag{12}$$

$$\langle w_{\mathrm{el}}(\underline{\mathbf{R}},t,\hat{\underline{\mathbf{k}}})\rangle = \tfrac{1}{4}\rho\omega^2\underline{\mathbf{u}}(\underline{\mathbf{R}},\omega,\hat{\underline{\mathbf{k}}})\cdot\underline{\mathbf{u}}^{*}(\underline{\mathbf{R}},\omega,\hat{\underline{\mathbf{k}}}) + \tfrac{1}{4}\underline{\underline{\mathbf{S}}}(\underline{\mathbf{R}},\omega,\hat{\underline{\mathbf{k}}}) : \underline{\underline{\underline{\mathbf{c}}}} : \underline{\underline{\mathbf{S}}}^{*}(\underline{\mathbf{R}},\omega,\hat{\underline{\mathbf{k}}}), \tag{13}$$

the star indicates complex conjugate values of Fourier-spectra. For homogeneous plane waves and

$$\underline{\underline{\mathbf{S}}}(\underline{\mathbf{R}},\omega,\hat{\underline{\mathbf{k}}}) = \mathrm{j}\frac{\omega}{c(\hat{\underline{\mathbf{k}}})}\underline{\underline{\underline{\mathbf{I}}}}^{+} : \hat{\underline{\mathbf{k}}}\,\underline{\mathbf{u}}(\underline{\mathbf{R}},\omega,\hat{\underline{\mathbf{k}}}), \tag{14}$$

we obtain the result

$$\underline{\mathbf{c}}_{\mathrm{E}}(\hat{\underline{\mathbf{k}}}) = \frac{1}{\rho c(\hat{\underline{\mathbf{k}}})}\underline{\underline{\underline{\mathbf{c}}}}\vdots\hat{\underline{\mathbf{k}}}\,\hat{\underline{\mathbf{u}}}(\hat{\underline{\mathbf{k}}})\hat{\underline{\mathbf{u}}}(\hat{\underline{\mathbf{k}}}). \tag{15}$$

Defining the slowness vector

$$\underline{\mathbf{s}}(\hat{\underline{\mathbf{k}}}) = \frac{1}{c(\hat{\underline{\mathbf{k}}})}\hat{\underline{\mathbf{k}}}, \tag{16}$$

and the ray vector

$$\underline{\mathbf{l}}(\hat{\underline{\mathbf{k}}}) = \frac{\underline{\mathbf{c}}_{\mathrm{E}}(\hat{\underline{\mathbf{k}}})}{\omega}, \tag{17}$$

one finds that the ray vector is always orthogonal to the slowness surface and the slowness vector is always orthogonal to the ray surface.

If it is physically reasonable to define a group velocity $\underline{\mathbf{c}}_g(\hat{\underline{\mathbf{k}}})$ in terms of

$$\underline{\mathbf{c}}_g(\hat{\underline{\mathbf{k}}}) = \nabla_{\underline{\mathbf{k}}}\omega(\underline{\mathbf{k}}), \tag{18}$$

with

$$\underline{\mathbf{k}} = \frac{\omega}{c(\hat{\underline{\mathbf{k}}})}\hat{\underline{\mathbf{k}}}, \tag{19}$$

the computation of this expression yields always the same result as (15). This is readily realized if the eigenvalue equation (9) is rewritten as—$\underline{\underline{\mathbf{I}}}$ is the second rank unit-tensor

$$[\underline{\mathbf{k}} \cdot \underline{\underline{\underline{\mathbf{c}}}} \cdot \underline{\mathbf{k}} - \rho\omega^2(\underline{\mathbf{k}})\underline{\underline{\mathbf{I}}}] \cdot \hat{\underline{\mathbf{u}}}(\hat{\underline{\mathbf{k}}}) = \underline{\mathbf{0}}, \tag{20}$$

and the $\nabla_{\underline{\mathbf{k}}}$-gradient of it is taken:

$$\begin{aligned}\nabla_{\underline{\mathbf{k}}}\{[\underline{\mathbf{k}} \cdot \underline{\underline{\underline{\mathbf{c}}}} \cdot \underline{\mathbf{k}} - \rho\omega^2(\underline{\mathbf{k}})\underline{\underline{\mathbf{I}}}] \cdot \hat{\underline{\mathbf{u}}}(\hat{\underline{\mathbf{k}}})\} &= \{\nabla_{\underline{\mathbf{k}}}[\underline{\mathbf{k}} \cdot \underline{\underline{\underline{\mathbf{c}}}} \cdot \underline{\mathbf{k}} - \rho\omega^2(\underline{\mathbf{k}})\underline{\underline{\mathbf{I}}}]\} \cdot \hat{\underline{\mathbf{u}}}(\underline{\mathbf{k}}) + [\nabla_{\underline{\mathbf{k}}}\hat{\underline{\mathbf{u}}}(\underline{\mathbf{k}})] \cdot [\underline{\mathbf{k}} \cdot \underline{\underline{\underline{\mathbf{c}}}} \cdot \underline{\mathbf{k}} - \rho\omega^2(\underline{\mathbf{k}})\underline{\underline{\mathbf{I}}}]^{21} \\ &= 2[\underline{\underline{\underline{\mathbf{c}}}} \cdot \underline{\mathbf{k}} - \rho\omega(\underline{\mathbf{k}})\nabla_{\underline{\mathbf{k}}}\omega(\underline{\mathbf{k}})\underline{\underline{\mathbf{I}}}] \cdot \hat{\underline{\mathbf{u}}}(\underline{\mathbf{k}}) + [\nabla_{\underline{\mathbf{k}}}\hat{\underline{\mathbf{u}}}(\hat{\underline{\mathbf{k}}})] \cdot [\underline{\mathbf{k}} \cdot \underline{\underline{\underline{\mathbf{c}}}} \cdot \underline{\mathbf{k}} - \rho\omega^2(\underline{\mathbf{k}})\underline{\underline{\mathbf{I}}}] = \underline{\mathbf{0}},\end{aligned} \tag{21}$$

we have used $\nabla_{\underline{\mathbf{k}}}\underline{\mathbf{k}} = \underline{\underline{\mathbf{I}}}$, $\nabla_{\underline{\mathbf{k}}}(\underline{\mathbf{k}} \cdot \underline{\underline{\underline{\mathbf{c}}}} \cdot \underline{\mathbf{k}}) = 2\underline{\underline{\underline{\mathbf{c}}}} \cdot \underline{\mathbf{k}}$ and the symmetries of $\underline{\underline{\underline{\mathbf{c}}}}$. Contracting (21) from the right with $\hat{\underline{\mathbf{u}}}(\hat{\underline{\mathbf{k}}})$ and recognizing again the eigenvalue equation results in

$$\underline{\underline{\underline{\mathbf{c}}}} \vdots \underline{\mathbf{k}}\hat{\underline{\mathbf{u}}}(\hat{\underline{\mathbf{k}}})\hat{\underline{\mathbf{u}}}(\hat{\underline{\mathbf{k}}}) = \rho\omega(\underline{\mathbf{k}})\nabla_{\underline{\mathbf{k}}}\omega(\underline{\mathbf{k}}), \tag{22}$$

and, hence, in

$$\underline{\mathbf{c}}_{\mathrm{E}}(\hat{\underline{\mathbf{k}}}) = \underline{\mathbf{c}}_g(\hat{\underline{\mathbf{k}}}). \tag{23}$$

Note: Even though irrelevant for the final result, the $\hat{\underline{\mathbf{k}}}$-dependence of $\hat{\underline{\mathbf{u}}}(\hat{\underline{\mathbf{k}}})$ must be considered taking the $\nabla_{\underline{\mathbf{k}}}$-gradient in the evaluation of (21); this is often disregarded in the literature (for instance: [13]).

2.2.2. Inhomogeneous plane waves

If we allow for complex phase vectors

$$\underline{\mathbf{k}} = \Re\underline{\mathbf{k}} + \mathrm{j}\Im\underline{\mathbf{k}}, \tag{24}$$

in the plane wave ansatz (8), we get

$$\underline{\mathbf{u}}(\mathbf{R}, \omega, \underline{\mathbf{k}}) = u(\omega)\mathrm{e}^{\mathrm{j}\Re\underline{\mathbf{k}}\cdot\mathbf{R}}\mathrm{e}^{-\Im\underline{\mathbf{k}}\cdot\mathbf{R}}\hat{\underline{\mathbf{u}}}(\underline{\mathbf{k}}), \tag{25}$$

which is called an *inhomogeneous* plane wave if $\Re\underline{\mathbf{k}}$ and $\Im\underline{\mathbf{k}}$ are not parallel; with our sign in the kernel of the Fourier transform, the phase of this wave propagates into $\Re\underline{\mathbf{k}}$-direction, and it decays exponentially in the half-

space $\Im\underline{\mathbf{k}}\cdot\underline{\mathbf{R}}>0$. The determinant of the wave tensor $\underline{\mathbf{k}}\cdot\underline{\underline{\underline{\mathbf{c}}}}\cdot\underline{\mathbf{k}}-\rho\omega^2\underline{\underline{\mathbf{I}}}$ in (20) is only zero if its real *and* imaginary part is zero for each wave mode (pressure and shear), yielding

$$\Im\underline{\mathbf{k}}\cdot\Re\underline{\mathbf{k}}=0, \tag{26}$$

for *isotropic lossless* materials, i.e. a potential exponential decay of a plane wave in such a material is always orthogonal to the *phase* propagation direction, and, hence, orthogonal to the phase velocity vector (as it is also true for electromagnetic waves: [10])

$$\underline{\mathbf{c}}(\underline{\mathbf{k}})=\frac{\omega}{|\Re\underline{\mathbf{k}}|}\,\widehat{\Re\underline{\mathbf{k}}}. \tag{27}$$

Of course, for *anisotropic lossless* materials one expects, that the orthogonal evanescence of inhomogeneous plane waves is with regard to the energy velocity vector. To prove this, we switch to the (complex) slowness vector $\underline{\mathbf{s}}=\Re\underline{\mathbf{s}}+\mathrm{j}\Im\underline{\mathbf{s}}=\underline{\mathbf{k}}/\omega$ and find

$$\underline{\mathbf{S}}_{\mathrm{K}}(\underline{\mathbf{R}},\omega,\underline{\mathbf{s}})=\tfrac{1}{2}\omega^2|u(\omega)|^2\mathrm{e}^{-2\omega\Im\underline{\mathbf{s}}\cdot\underline{\mathbf{R}}}\underline{\hat{\mathbf{u}}}(\underline{\mathbf{s}})\cdot\underline{\underline{\underline{\mathbf{c}}}}:\underline{\mathbf{s}}^*\underline{\hat{\mathbf{u}}}^*(\underline{\mathbf{s}}), \tag{28}$$

$$\langle w(\underline{\mathbf{R}},t,\underline{\mathbf{s}})\rangle=\tfrac{1}{4}\omega^2|u(\omega)|^2\mathrm{e}^{-2\omega\Im\underline{\mathbf{s}}\cdot\underline{\mathbf{R}}}[\rho+\underline{\mathbf{s}}\,\underline{\hat{\mathbf{u}}}(\underline{\mathbf{s}}):\underline{\underline{\underline{\mathbf{c}}}}:\underline{\mathbf{s}}^*\underline{\hat{\mathbf{u}}}^*(\underline{\mathbf{s}})], \tag{29}$$

from (12) and (13), where we have used the hermitian normalization condition

$$\underline{\hat{\mathbf{u}}}(\underline{\mathbf{s}})\cdot\underline{\hat{\mathbf{u}}}^*(\underline{\mathbf{s}})=1, \tag{30}$$

(29) implies that time averaged potential and kinetic energy densities are no longer equal for *inhomogeneous* time-harmonic plane waves (as it is true for homogeneous plane waves). According to (11) we obtain

$$\underline{\mathbf{c}}_{\mathrm{E}}(\underline{\mathbf{s}})=\frac{2\Re\{\underline{\underline{\underline{\mathbf{c}}}}\vdots\underline{\mathbf{s}}^*\underline{\hat{\mathbf{u}}}^*(\underline{\mathbf{s}})\underline{\hat{\mathbf{u}}}(\underline{\mathbf{s}})\}}{\rho+\underline{\mathbf{s}}\,\underline{\hat{\mathbf{u}}}(\underline{\mathbf{s}}):\underline{\underline{\underline{\mathbf{c}}}}:\underline{\mathbf{s}}^*\underline{\hat{\mathbf{u}}}^*(\underline{\mathbf{s}})}. \tag{31}$$

Calculating

$$\Re\{\underline{\underline{\underline{\mathbf{c}}}}\vdots\underline{\mathbf{s}}^*\underline{\hat{\mathbf{u}}}^*\underline{\hat{\mathbf{u}}}\}=\underline{\underline{\underline{\mathbf{c}}}}\vdots(\Re\underline{\mathbf{s}}\,\Re\underline{\hat{\mathbf{u}}}\,\Re\underline{\hat{\mathbf{u}}}+\Re\underline{\mathbf{s}}\,\Im\underline{\hat{\mathbf{u}}}\,\Im\underline{\hat{\mathbf{u}}}+\Im\underline{\mathbf{s}}\,\Re\underline{\hat{\mathbf{u}}}\,\Im\underline{\hat{\mathbf{u}}}-\Im\underline{\mathbf{s}}\,\Im\underline{\hat{\mathbf{u}}}\,\Re\underline{\hat{\mathbf{u}}}), \tag{32}$$

explicitly in terms of the real and imaginary part of $\underline{\mathbf{s}}$, we find

$$\Im\underline{\mathbf{s}}\cdot\Re\{\underline{\underline{\underline{\mathbf{c}}}}\vdots\underline{\mathbf{s}}^*\underline{\hat{\mathbf{u}}}^*\underline{\hat{\mathbf{u}}}\}=\Im\underline{\mathbf{s}}\cdot\underline{\underline{\underline{\mathbf{c}}}}\vdots(\Re\underline{\mathbf{s}}\,\Re\underline{\hat{\mathbf{u}}}\,\Re\underline{\hat{\mathbf{u}}}+\Re\underline{\mathbf{s}}\,\Im\underline{\hat{\mathbf{u}}}\,\Im\underline{\hat{\mathbf{u}}}), \tag{33}$$

on behalf of the symmetries of $\underline{\underline{\underline{\mathbf{c}}}}$; we expect the right-hand side of (33) to be zero. This is recognized, if we conclude

$$\Im\{\underline{\mathbf{s}}^*\cdot\underline{\underline{\underline{\mathbf{c}}}}\vdots\underline{\mathbf{s}}^*\underline{\hat{\mathbf{u}}}^*\underline{\hat{\mathbf{u}}}\}=0, \tag{34}$$

from the dot-multiplication of the complex conjugate of the eigenvalue equation (20) with $\underline{\hat{\mathbf{u}}}(\underline{\mathbf{s}})$ exploiting (30); again, based on the symmetries of $\underline{\underline{\underline{\mathbf{c}}}}$, we find explicitly

$$\Im\{\underline{\mathbf{s}}^*\cdot\underline{\underline{\underline{\mathbf{c}}}}\vdots\underline{\mathbf{s}}^*\underline{\hat{\mathbf{u}}}^*\underline{\hat{\mathbf{u}}}\}=2\Im\underline{\mathbf{s}}\cdot\underline{\underline{\underline{\mathbf{c}}}}\vdots(\Re\underline{\mathbf{s}}\Re\underline{\hat{\mathbf{u}}}\Re\underline{\hat{\mathbf{u}}}+\Re\underline{\mathbf{s}}\Im\underline{\hat{\mathbf{u}}}\Im\underline{\hat{\mathbf{u}}}), \tag{35}$$

and, hence,

$$\Im\underline{\mathbf{s}}\cdot\underline{\mathbf{c}}_{\mathrm{E}}(\underline{\mathbf{s}})=0. \tag{36}$$

2.3. Transversely isotropic materials

2.3.1. Phase wave speeds

Transverse isotropy is characterized by a unit-vector preference direction $\underline{\hat{\mathbf{a}}}$—the grain orientation in an austenitic weld—along which the material is anistropic whereas orthogonal to $\underline{\hat{\mathbf{a}}}$ it is isotropic. The corresponding stiffness tensor, which involves five Lamé constants $\lambda_\perp$, $\lambda_\parallel$, $\mu_\perp$, $\mu_\parallel$, ν, reads [9]

$$\underline{\underline{\underline{\underline{\mathbf{c}}}}}^{\text{triso}} = \lambda_\perp \underline{\underline{\underline{\underline{\mathbf{I}}}}}^{\delta} + 2\mu_\perp \underline{\underline{\underline{\underline{\mathbf{I}}}}}^{+} + \alpha_1 \underline{\hat{\mathbf{a}}}\,\underline{\hat{\mathbf{a}}}\,\underline{\hat{\mathbf{a}}}\,\underline{\hat{\mathbf{a}}} + \alpha_2(\underline{\mathbf{I}}\,\underline{\hat{\mathbf{a}}}\,\underline{\hat{\mathbf{a}}} + \underline{\hat{\mathbf{a}}}\,\underline{\hat{\mathbf{a}}}\,\underline{\mathbf{I}}) + \alpha_3(\underline{\mathbf{I}}\,\underline{\hat{\mathbf{a}}}\,\underline{\hat{\mathbf{a}}} + \underline{\hat{\mathbf{a}}}\,\underline{\hat{\mathbf{a}}}\,\underline{\mathbf{I}})^{1324} + \alpha_3(\underline{\mathbf{I}}\,\underline{\hat{\mathbf{a}}}\,\underline{\hat{\mathbf{a}}} + \underline{\hat{\mathbf{a}}}\,\underline{\hat{\mathbf{a}}}\,\underline{\mathbf{I}})^{1342}, \quad (37)$$

where

$$\alpha_1 = \lambda_\perp + 2\mu_\perp + \lambda_\parallel + 2\mu_\parallel - 2(\nu + 2\mu_\parallel), \quad (38)$$

$$\alpha_2 = \nu - \lambda_\perp, \quad (39)$$

$$\alpha_3 = \mu_\parallel - \mu_\perp, \quad (40)$$

$\underline{\underline{\underline{\underline{\mathbf{I}}}}}^{\delta} = \underline{\underline{\mathbf{II}}}$ has the property $\underline{\underline{\underline{\underline{\mathbf{I}}}}}^{\delta} : \underline{\underline{\mathbf{A}}} = \underline{\underline{\mathbf{A}}} : \underline{\underline{\underline{\underline{\mathbf{I}}}}}^{\delta} = \underline{\underline{\mathbf{A}}}\text{trace}\underline{\underline{\mathbf{A}}}$. The wave tensor in (20) immediately takes the form

$$\underline{\underline{\mathbf{W}}}(\underline{\hat{\mathbf{k}}}, c^2) = \underline{\hat{\mathbf{k}}} \cdot \underline{\underline{\underline{\underline{\mathbf{c}}}}} \cdot \underline{\hat{\mathbf{k}}} - \rho\, c^2(\underline{\hat{\mathbf{k}}})\underline{\mathbf{I}} = \gamma_1 \underline{\mathbf{I}} + \gamma_2 \underline{\hat{\mathbf{k}}}\,\underline{\hat{\mathbf{k}}} + \gamma_3 \underline{\hat{\mathbf{a}}}\,\underline{\hat{\mathbf{a}}} + \gamma_4(\underline{\hat{\mathbf{k}}}\,\underline{\hat{\mathbf{a}}} + \underline{\hat{\mathbf{a}}}\,\underline{\hat{\mathbf{k}}}), \quad (41)$$

where

$$\gamma_1 = \mu_\perp + (\mu_\parallel - \mu_\perp)(\underline{\hat{\mathbf{k}}} \cdot \underline{\hat{\mathbf{a}}})^2 - \rho c^2(\underline{\hat{\mathbf{k}}}), \quad (42)$$

$$\gamma_2 = \lambda_\perp + \mu_\perp, \quad (43)$$

$$\gamma_3 = (\lambda_\perp + 2\mu_\perp + \lambda_\parallel - 2\mu_\parallel - 2\nu)(\underline{\hat{\mathbf{k}}} \cdot \underline{\hat{\mathbf{a}}})^2 + \mu_\parallel - \mu_\perp, \quad (44)$$

$$\gamma_4 = (\mu_\parallel - \mu_\perp + \nu - \lambda_\perp)\underline{\hat{\mathbf{k}}} \cdot \underline{\hat{\mathbf{a}}}. \quad (45)$$

The first task is to compute the $c^2(\underline{\hat{\mathbf{k}}})$-eigenvalues, which requires the computation of the determinant of $\underline{\underline{\mathbf{W}}}(\underline{\hat{\mathbf{k}}}, c^2)$; with the help of Chen's formulas [10] we find

$$\det\underline{\underline{\mathbf{W}}}(\underline{\hat{\mathbf{k}}}, c^2) = \gamma_1\{\gamma_1^2 + \gamma_1(\gamma_2 + \gamma_3 + 2\gamma_4 \underline{\hat{\mathbf{k}}} \cdot \underline{\hat{\mathbf{a}}}) + (\gamma_2\gamma_3 - \gamma_4^2)[1 - (\underline{\hat{\mathbf{k}}} \cdot \underline{\hat{\mathbf{a}}})^2]\}, \quad (46)$$

hence, the first eigenvalue is immediately obtained through $\gamma_1 = 0$ to yield

$$c^2_{\text{SH}}(\underline{\hat{\mathbf{k}}}) = \frac{\mu_\perp + (\mu_\parallel - \mu_\perp)(\underline{\hat{\mathbf{k}}} \cdot \underline{\hat{\mathbf{a}}})^2}{\rho}, \quad (47)$$

where the notation "SH" for shear horizontal anticipates the direction of the corresponding eigenvector: It is horizontal with regard to a plane being orthogonal to the $\underline{\hat{\mathbf{k}}}\,\underline{\hat{\mathbf{a}}}$-plane, and therefore orthogonal to $\underline{\hat{\mathbf{k}}}$ identifying the wave with the phase speed (47) as a transverse shear wave. The second and third eigenvalues come as a solution of the bracketed expression in (46), which is a quadratic equation in γ_1:

$$c^2_{\text{qP,qSV}}(\underline{\hat{\mathbf{k}}}) = c^2_{\text{SH}}(\underline{\hat{\mathbf{k}}}) - \frac{\gamma_1^{\text{qP,qSV}}}{\rho}, \quad (48)$$

$$= c^2_{\text{SH}}(\underline{\hat{\mathbf{k}}}) + \frac{1/2(\gamma_2 + \gamma_3 + 2\gamma_4 \underline{\hat{\mathbf{k}}} \cdot \underline{\hat{\mathbf{a}}})}{\rho} \pm \frac{1/2\sqrt{(\gamma_2 + \gamma_3 + 2\gamma_4\, \underline{\hat{\mathbf{k}}} \cdot \underline{\hat{\mathbf{a}}})^2 - 4(\gamma_2\gamma_3 - \gamma_4^2)[1 - (\underline{\hat{\mathbf{k}}} \cdot \underline{\hat{\mathbf{a}}})^2]}}{\rho}. \quad (49)$$

Again, the notation anticipates the direction of the corresponding polarization vectors: They are no longer longitudinal nor transverse with regard to $\underline{\hat{\mathbf{k}}}$, whence the "q" for quasi appears; in addition, for zero anisotropy one

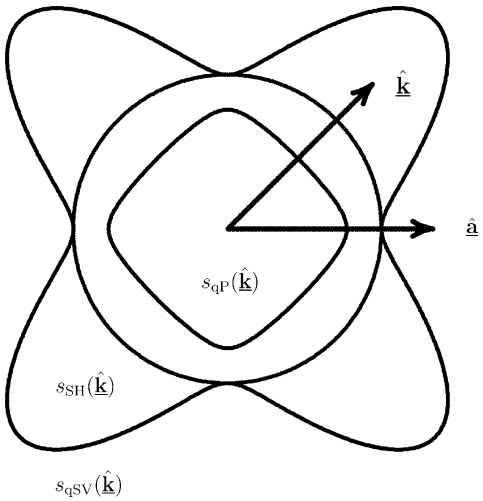

Fig. 4. *Slownesses* $s_{\mathrm{SH}}(\hat{\underline{\mathbf{k}}})$, $s_{\mathrm{qSV}}(\hat{\underline{\mathbf{k}}})$ and $s_{\mathrm{qP}}(\hat{\underline{\mathbf{k}}})$ for austenitic steel: $\lambda_\perp + 2\mu_\perp = 216\,\mathrm{GPa}$, $\mu_\perp = 129\,\mathrm{GPa}$, $\lambda_\parallel + 2\mu_\parallel = 216\,\mathrm{GPa}$, $\mu_\parallel = 129\,\mathrm{GPa}$, $\nu = 145\,\mathrm{GPa}$; $\rho = 8100\,\mathrm{kg/m^3}$.

eigenvalue refers to a pressure (P) and the other to a shear vertical (SV) wave, and this results in qP- and qSV-wave modes to complement the SH-mode. In Fig. 4 we have displayed the $\hat{\underline{\mathbf{k}}}$-dependence of the slowness magnitudes $s_{\mathrm{qP}}(\hat{\underline{\mathbf{k}}})$, $s_{\mathrm{SH}}(\hat{\underline{\mathbf{k}}})$, $s_{\mathrm{qSV}}(\hat{\underline{\mathbf{k}}})$ in the $\hat{\underline{\mathbf{k}}}\,\hat{\underline{\mathbf{a}}}$-plane for an austenitic steel with the Lamé constants and density given in the figure caption; these diagrams are rotationally symmetric with respect to $\hat{\underline{\mathbf{a}}}$. In general we have $s_{\mathrm{SH,qSV}}(\hat{\underline{\mathbf{k}}}) < s_{\mathrm{qP}}(\hat{\underline{\mathbf{k}}})$ (for exceptions see [13]); hence, "quasi" stands indeed for the polarization vectors (and the pressure and shear physics) and not for primary and secondary waves.

2.3.2. Polarization vectors

To compute the energy velocity we need the polarization vectors, i.e. the eigenvectors corresponding to each eigenvalue. We immediately observe that $\underline{\underline{\mathbf{W}}}(\hat{\underline{\mathbf{k}}}, c_{\mathrm{SH}}^2)$ is a sum of two dyadic products, and therefore, this tensor is planar [10]; as a consequence, its adjoint according to

$$\mathrm{adj}\underline{\underline{\mathbf{W}}}^{\mathrm{triso}}(\hat{\underline{\mathbf{k}}}, c_{\mathrm{SH}}^2) = (\gamma_2\gamma_3 - \gamma_4^2)(\hat{\underline{\mathbf{k}}} \times \hat{\underline{\mathbf{a}}})(\hat{\underline{\mathbf{k}}} \times \hat{\underline{\mathbf{a}}}), \tag{50}$$

is linear and the eigenvector $\hat{\underline{\mathbf{u}}}_{\mathrm{SH}}(\hat{\underline{\mathbf{k}}})$ is proportional to the left vector of the dyadic product (50); after normalization we obtain:

$$\hat{\underline{\mathbf{u}}}_{\mathrm{SH}}(\hat{\underline{\mathbf{k}}}) = \frac{\hat{\underline{\mathbf{k}}} \times \hat{\underline{\mathbf{a}}}}{\sqrt{1 - (\hat{\underline{\mathbf{k}}} \cdot \hat{\underline{\mathbf{a}}})^2}}, \tag{51}$$

thus confirming our anticipation that $\hat{\underline{\mathbf{u}}}_{\mathrm{SH}}$ is orthogonal to the $\hat{\underline{\mathbf{k}}}\,\hat{\underline{\mathbf{a}}}$-plane; yet this does not immediately explain the notation "SH" for shear horizontal: It only becomes reasonable if a reference plane, i.e. a specimen surface, is defined and if $\hat{\underline{\mathbf{k}}}$ and $\hat{\underline{\mathbf{a}}}$ span a plane orthogonal to it. The same is true for the notation "qSV" for shear vertical (Figs. 5 and 6).

The special case $\hat{\underline{\mathbf{k}}} \perp \hat{\underline{\mathbf{a}}}$ is contained in (50), but not $\hat{\underline{\mathbf{k}}} \parallel \hat{\underline{\mathbf{a}}}$, because

$$\mathrm{adj}\underline{\underline{\mathbf{W}}}^{\mathrm{triso}}(\hat{\underline{\mathbf{k}}} \parallel \hat{\underline{\mathbf{a}}}, c_{\mathrm{SH}}^2) = \underline{\mathbf{0}}, \tag{52}$$

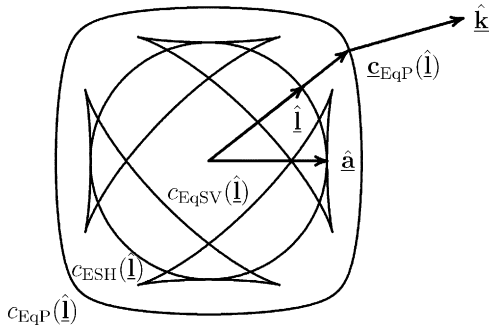

Fig. 5. Energy wave speeds $c_{\mathrm{ESH}}(\hat{\underline{\mathbf{k}}})$, $c_{\mathrm{EqSV}}(\hat{\underline{\mathbf{k}}})$ and $c_{\mathrm{EqP}}(\hat{\underline{\mathbf{k}}})$ for austenitic steel: $\lambda_\perp + 2\mu_\perp = 216\,\mathrm{GPa}$, $\mu_\perp = 129\,\mathrm{GPa}$, $\lambda_\parallel + 2\mu_\parallel = 216\,\mathrm{GPa}$, $\mu_\parallel = 129\,\mathrm{GPa}$, $\nu = 145\,\mathrm{GPa}$; $\rho = 8100\,\mathrm{kg/m^3}$.

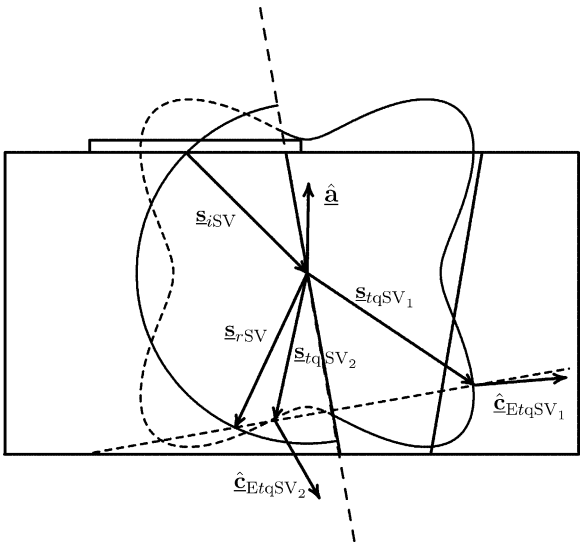

Fig. 6. Excitation of two qSV-wave modes in an austenitic weld by a 45°-SV transducer.

is the null tensor; as a consequence $\underline{\underline{\mathbf{W}}}^{\mathrm{triso}}(\hat{\underline{\mathbf{k}}}\|\hat{\underline{\mathbf{a}}}, c_{\mathrm{SH}}^2)$ is linear:

$$\underline{\underline{\mathbf{W}}}^{\mathrm{triso}}(\hat{\underline{\mathbf{k}}}\|\hat{\underline{\mathbf{a}}}, c_{\mathrm{SH}}^2) = (\gamma_2 + \gamma_3 + 2\gamma_4)\hat{\underline{\mathbf{a}}}\,\hat{\underline{\mathbf{a}}}, \tag{53}$$

therefore, the eigenvector $\hat{\underline{\mathbf{u}}}_{\mathrm{SH}}(\hat{\underline{\mathbf{k}}}\|\hat{\underline{\mathbf{a}}})$ is proportional to any vector orthogonal to the right vector $\hat{\underline{\mathbf{a}}}$ of the dyadic (53).

Knowing that the Kelvin–Christoffel tensor is real-symmetric, we conclude that the remaining two eigenvectors must be orthogonal to $\hat{\underline{\mathbf{u}}}_{\mathrm{SH}}$ and orthogonal to each other. This requires

$$\hat{\underline{\mathbf{u}}}_{\mathrm{qP,qSV}}(\hat{\underline{\mathbf{k}}}) \sim \alpha_{\mathrm{qP,qSV}}\hat{\underline{\mathbf{k}}} + \beta_{\mathrm{qP,qSV}}\hat{\underline{\mathbf{a}}}, \tag{54}$$

we determine $\beta_{\mathrm{qP,qSV}}/\alpha_{\mathrm{qP,qSV}}$ inserting (54) into the eigenvalue equation which results in a homogeneous system of equations whose determinant is found to be zero as a requirement for a non-trivial solution to exist. We find

$$\frac{\beta_{\mathrm{qP,qSV}}}{\alpha_{\mathrm{qP,qSV}}} \stackrel{\mathrm{def}}{=} \gamma_{\mathrm{qP,qSV}} = -\frac{\gamma_1^{\mathrm{qP,qSV}} + \gamma_2 + \gamma_4\hat{\underline{\mathbf{k}}}\cdot\hat{\underline{\mathbf{a}}}}{\gamma_4 + \gamma_2\,\hat{\underline{\mathbf{k}}}\cdot\hat{\underline{\mathbf{a}}}} = -\frac{\rho c_{\mathrm{SH}}^2 - \rho c_{\mathrm{qP,qSV}}^2 + \gamma_2 + \gamma_4\hat{\underline{\mathbf{k}}}\cdot\hat{\underline{\mathbf{a}}}}{(\nu + \mu_\parallel)\hat{\underline{\mathbf{k}}}\cdot\hat{\underline{\mathbf{a}}}}, \tag{55}$$

and therefore

$$\hat{\underline{\mathbf{u}}}_{\mathrm{qP,qSV}}(\hat{\underline{\mathbf{k}}}) = \frac{\hat{\underline{\mathbf{k}}} - \left[1/2(\gamma_2-\gamma_3) \mp 1/2\sqrt{(\gamma_2+\gamma_3+2\gamma_4\hat{\underline{\mathbf{k}}}\cdot\hat{\underline{\mathbf{a}}})^2 - 4(\gamma_2\gamma_3-\gamma_4^2)[1-(\hat{\underline{\mathbf{k}}}\cdot\hat{\underline{\mathbf{a}}})^2]}\right]\hat{\underline{\mathbf{a}}}/(\gamma_4+\gamma_2\,\hat{\underline{\mathbf{k}}}\cdot\hat{\underline{\mathbf{a}}})}{U_{\mathrm{qP,qSV}}} \tag{56}$$

with

$$U_{\mathrm{qP,qSV}} = |\hat{\underline{\mathbf{k}}} + \gamma_{\mathrm{qP,qSV}}\hat{\underline{\mathbf{a}}}| = \sqrt{1+\gamma_{\mathrm{qP,qSV}}^2 + 2\gamma_{\mathrm{qP,qSV}}\hat{\underline{\mathbf{k}}}\cdot\hat{\underline{\mathbf{a}}}}. \tag{57}$$

A short calculation proves indeed that

$$\hat{\underline{\mathbf{u}}}_{\mathrm{qP}}(\hat{\underline{\mathbf{k}}})\cdot\hat{\underline{\mathbf{u}}}_{\mathrm{qSV}}(\hat{\underline{\mathbf{k}}}) = 0. \tag{58}$$

For the special case $\hat{\underline{\mathbf{k}}}\cdot\hat{\underline{\mathbf{a}}} = 0$ we have $\gamma_4 = 0$, and, hence, (56) cannot be used; but then we find

$$\mathrm{adj}\,\underline{\underline{\mathbf{W}}}^{\mathrm{triso}}(\hat{\underline{\mathbf{k}}}\perp\hat{\underline{\mathbf{a}}}, c_{\mathrm{qP}}^2) = \gamma_2(\gamma_2-\gamma_3)\hat{\underline{\mathbf{k}}}\,\hat{\underline{\mathbf{k}}}, \tag{59}$$

$$\mathrm{adj}\,\underline{\underline{\mathbf{W}}}^{\mathrm{triso}}(\hat{\underline{\mathbf{k}}}\perp\hat{\underline{\mathbf{a}}}, c_{\mathrm{qSV}}^2) = \gamma_3(\gamma_3-\gamma_2)\hat{\underline{\mathbf{a}}}\,\hat{\underline{\mathbf{a}}}, \tag{60}$$

yielding the result that $\hat{\underline{\mathbf{u}}}_{\mathrm{qP}}(\hat{\underline{\mathbf{k}}}\perp\hat{\underline{\mathbf{a}}})$ is parallel to $\hat{\underline{\mathbf{k}}}$ and $\hat{\underline{\mathbf{u}}}_{\mathrm{qSV}}(\hat{\underline{\mathbf{k}}}\perp\hat{\underline{\mathbf{a}}})$ parallel to $\hat{\underline{\mathbf{a}}}$. For the other special case $\hat{\underline{\mathbf{k}}}\times\hat{\underline{\mathbf{a}}} = \underline{\mathbf{0}}$, $\hat{\underline{\mathbf{k}}}$ and $\hat{\underline{\mathbf{a}}}$ are not linearly independent, and, therefore, our derivation does not hold. Yet we find that $\mathrm{adj}\,\underline{\underline{\mathbf{W}}}^{\mathrm{triso}}(\hat{\underline{\mathbf{k}}}\|\hat{\underline{\mathbf{a}}}, c_{\mathrm{SH,qSV}}^2)$ is the null tensor with the consequence that

$$\underline{\underline{\mathbf{W}}}^{\mathrm{triso}}(\hat{\underline{\mathbf{k}}}\|\hat{\underline{\mathbf{a}}}, c_{\mathrm{SH,qSV}}^2) = (\gamma_2+\gamma_3+2\gamma_4)\hat{\underline{\mathbf{a}}}\,\hat{\underline{\mathbf{a}}}, \tag{61}$$

is linear and $\hat{\underline{\mathbf{u}}}_{\mathrm{SH,qSV}}(\hat{\underline{\mathbf{k}}}\,\hat{\underline{\mathbf{a}}})$ orthogonal to the right factor $\hat{\underline{\mathbf{a}}}$: We choose $\hat{\underline{\mathbf{u}}}_{\mathrm{SH}}$ and $\hat{\underline{\mathbf{u}}}_{\mathrm{qSV}}$ orthogonal to each other as we do it for the case of equal shear eigenvalues in isotropic materials. In addition we have

$$\mathrm{adj}\,\underline{\underline{\mathbf{W}}}^{\mathrm{triso}}(\hat{\underline{\mathbf{k}}}\|\hat{\underline{\mathbf{a}}}, c_{\mathrm{qP}}^2) \sim \hat{\underline{\mathbf{a}}}\,\hat{\underline{\mathbf{a}}}, \tag{62}$$

therefore, $\hat{\underline{\mathbf{u}}}_{\mathrm{qP}}(\hat{\underline{\mathbf{k}}}\|\hat{\underline{\mathbf{a}}})$ is parallel to the left vector $\hat{\underline{\mathbf{a}}}$.

Note that the explicit coordinate-free eigenvector expressions given here turn out to be considerably simpler than those given in the literature [9], where Chen's formulas ([10]: Problem 1.12) for the eigenvectors of a biaxial matrix are used.

2.3.3. Energy wave speeds

With the stiffness tensor for transversely isotropic materials we find the general expression

$$\begin{aligned}\underline{\mathbf{c}}_{\mathrm{E}}(\hat{\underline{\mathbf{k}}}) = \frac{1}{\rho\, c(\hat{\underline{\mathbf{k}}})}[&\lambda_\perp\hat{\underline{\mathbf{k}}}\cdot\hat{\underline{\mathbf{u}}}\,\hat{\underline{\mathbf{u}}} + \mu_\perp\hat{\underline{\mathbf{k}}} + \mu_\perp\hat{\underline{\mathbf{k}}}\cdot\hat{\underline{\mathbf{u}}}\,\hat{\underline{\mathbf{u}}} + \alpha_1\hat{\underline{\mathbf{k}}}\cdot\hat{\underline{\mathbf{a}}}(\hat{\underline{\mathbf{u}}}\cdot\hat{\underline{\mathbf{a}}})^2\hat{\underline{\mathbf{a}}} + \alpha_2(\hat{\underline{\mathbf{k}}}\cdot\hat{\underline{\mathbf{a}}}\,\hat{\underline{\mathbf{a}}}\cdot\hat{\underline{\mathbf{u}}}\,\hat{\underline{\mathbf{u}}} + \hat{\underline{\mathbf{k}}}\cdot\hat{\underline{\mathbf{u}}}\,\hat{\underline{\mathbf{u}}}\cdot\hat{\underline{\mathbf{a}}}\,\hat{\underline{\mathbf{a}}})\\ &+\alpha_3(\hat{\underline{\mathbf{k}}}\cdot\hat{\underline{\mathbf{a}}}\,\hat{\underline{\mathbf{a}}}\cdot\hat{\underline{\mathbf{u}}}\,\hat{\underline{\mathbf{u}}} + \hat{\underline{\mathbf{a}}}\cdot\hat{\underline{\mathbf{u}}}\,\hat{\underline{\mathbf{u}}}\cdot\hat{\underline{\mathbf{k}}}\,\hat{\underline{\mathbf{a}}} + \hat{\underline{\mathbf{u}}}\cdot\hat{\underline{\mathbf{a}}}\,\hat{\underline{\mathbf{a}}}\cdot\hat{\underline{\mathbf{u}}}\,\hat{\underline{\mathbf{k}}} + \hat{\underline{\mathbf{k}}}\cdot\hat{\underline{\mathbf{a}}}\,\hat{\underline{\mathbf{a}}})],\end{aligned} \tag{63}$$

for the energy wave speed. Specializing to the three different wave modes we get

$$\underline{\mathbf{c}}_{\mathrm{ESH}}(\hat{\underline{\mathbf{k}}}) = \frac{\mu_\perp\hat{\underline{\mathbf{k}}} + (\mu_\parallel-\mu_\perp)\hat{\underline{\mathbf{k}}}\cdot\hat{\underline{\mathbf{a}}}\,\hat{\underline{\mathbf{a}}}}{\rho\, c_{\mathrm{SH}}(\hat{\underline{\mathbf{k}}})}, \tag{64}$$

$$\rho\, c_{\mathrm{qP,qSV}}(\hat{\underline{\mathbf{k}}})\underline{\mathbf{c}}_{\mathrm{EqP,qSV}}(\hat{\underline{\mathbf{k}}}) = \Big\{\mu_\perp + \alpha_3\hat{\underline{\mathbf{u}}}_{\mathrm{qP,qSV}}\cdot\hat{\underline{\mathbf{a}}}\,\hat{\underline{\mathbf{a}}}\cdot\hat{\underline{\mathbf{u}}}_{\mathrm{qP,qSV}}$$
$$+ \frac{1}{U_{\mathrm{qP,qSV}}}[(\lambda_\perp+\mu_\perp)\hat{\underline{\mathbf{k}}}\cdot\hat{\underline{\mathbf{u}}}_{\mathrm{qP,qSV}} + (\alpha_2+\alpha_3)\hat{\underline{\mathbf{k}}}\cdot\hat{\underline{\mathbf{a}}}\,\hat{\underline{\mathbf{a}}}\cdot\hat{\underline{\mathbf{u}}}_{\mathrm{qP,qSV}}]\Big\}\,\hat{\underline{\mathbf{k}}}$$
$$+ \Big\{(\alpha_1\hat{\underline{\mathbf{k}}}\cdot\hat{\underline{\mathbf{a}}}\,\hat{\underline{\mathbf{a}}}\cdot\hat{\underline{\mathbf{u}}}_{\mathrm{qP,qSV}} + \alpha_2\hat{\underline{\mathbf{k}}}\cdot\hat{\underline{\mathbf{u}}}_{\mathrm{qP,qSV}})\hat{\underline{\mathbf{u}}}_{\mathrm{qP,qSV}}\cdot\hat{\underline{\mathbf{a}}} + \alpha_3(\hat{\underline{\mathbf{k}}}\cdot\hat{\underline{\mathbf{a}}}$$
$$+ \hat{\underline{\mathbf{k}}}\cdot\hat{\underline{\mathbf{u}}}_{\mathrm{qP,qSV}}\hat{\underline{\mathbf{u}}}_{\mathrm{qP,qSV}}\cdot\hat{\underline{\mathbf{a}}}) + \frac{\gamma_{\mathrm{qP,qSV}}}{U_{\mathrm{qP,qSV}}}[(\lambda_\perp+\mu_\perp)\hat{\underline{\mathbf{k}}}\cdot\hat{\underline{\mathbf{u}}}_{\mathrm{qP,qSV}}$$
$$+ (\alpha_2+\alpha_3)\hat{\underline{\mathbf{k}}}\cdot\hat{\underline{\mathbf{a}}}\,\hat{\underline{\mathbf{a}}}\cdot\hat{\underline{\mathbf{u}}}_{\mathrm{qP,qSV}}]\Big\}\,\hat{\underline{\mathbf{a}}}. \tag{65}$$

To plot energy velocity diagrams (see Fig. 5) in a manner similar to the slowness diagrams we choose $\hat{\underline{\mathbf{k}}}$ and plot $|\underline{\mathbf{c}}_{\mathrm{ESH,qP,qSV}}(\hat{\underline{\mathbf{k}}})|$ in the direction of the unit-ray-vector $\hat{\underline{\mathbf{l}}}(\hat{\underline{\mathbf{k}}}) = \hat{\underline{\mathbf{c}}}_{\mathrm{ESH,qP,qSV}}(\hat{\underline{\mathbf{k}}})$; due to the potential non-uniqueness of $\hat{\underline{\mathbf{k}}}(\hat{\underline{\mathbf{l}}})$ the typical cusps in the $c_{\mathrm{EqSV}}(\hat{\underline{\mathbf{l}}})$ diagram appear [16]. Interesting enough: The geometrical shapes of the *plane wave energy velocity diagrams* are identical to the transient wave fronts emanating from point sources, i.e. to the transient Huygens-type elementary waves, and, hence, *wave fronts of transient Green functions*, yet without the vector/tensor and amplitude information of the latter [15,16,3,6]. Nevertheless, this gives rise to a point source synthesis of transducer radiation fields [17] as well as an imaging scheme based on time domain backpropagation [4,14].

As a consequence, it is absolutely inappropriate to take the inverse Fourier transform of the time harmonic plane wave (8) to arrive at a transient plane wave; in contrast, one has to define a *transient plane wave energy ray* (propagating into positive $\hat{\underline{\mathbf{l}}}$-direction) according to

$$\underline{\mathbf{u}}(\underline{\mathbf{R}}, t, \hat{\underline{\mathbf{l}}}) = U\left(t - \frac{\hat{\underline{\mathbf{l}}}\cdot\underline{\mathbf{R}}}{c_{\mathrm{E}}(\hat{\underline{\mathbf{l}}})}\right)\hat{\underline{\mathbf{u}}}(\hat{\underline{\mathbf{l}}}), \tag{66}$$

where $U(t)$ is the inverse Fourier transform of $u(\omega)$.

3. Transmission of transient plane wave energy rays at the plane boundary separating a transversely isotropic from an isotropic half-space

We discuss this topic for the special case of SV-wave incidence from the isotropic half-space because of its relevance for the weld example in Fig. 2. As a matter of fact, we "insert" in Fig. 6 the $s_{\mathrm{qSV}}(\hat{\underline{\mathbf{k}}})$-slowness diagram of Fig. 4 into the zero-order computer model weld geometry of Fig. 1 together with the circular s_{SV}-diagram for the isotropic half-space. The slowness vector $\underline{\mathbf{s}}_{i\mathrm{SV}}$ of the incident wave determines the slowness vector $\underline{\mathbf{s}}_{r\mathrm{SV}}$ of the reflected SV-wave via phase matching in the interface between the ferritic and the austenitic steel, thus defining the (dashed) phase matching line for the transmitted shear wave: It has four intersections with the corresponding qSV-slowness diagram, two of which lead to non-evanescent energy velocity directions $\hat{\underline{\mathbf{l}}}_{1,2} = \hat{\underline{\mathbf{c}}}_{t\mathrm{qSV}_{1,2}}$ pointing *into* the transversely isotropic half-space and leading to *two* transmitted transient plane $\mathrm{qSV}_{t_{1,2}}$-wave energy rays (the mode-converted transmitted qP-wave is already way beyond evanescence in the sense of (36)):

$$\underline{\mathbf{u}}_{t\mathrm{qSV}_{1,2}}(\underline{\mathbf{R}}, t, \hat{\underline{\mathbf{l}}}_{1,2}) = U\left(t - \frac{\hat{\underline{\mathbf{l}}}_{1,2}\cdot\underline{\mathbf{R}}}{c_{\mathrm{E}t\mathrm{qSV}_{1,2}}(\hat{\underline{\mathbf{l}}}_{1,2})}\right)\hat{\underline{\mathbf{u}}}_{t\mathrm{qSV}_{1,2}}(\hat{\underline{\mathbf{l}}}_{1,2}). \tag{67}$$

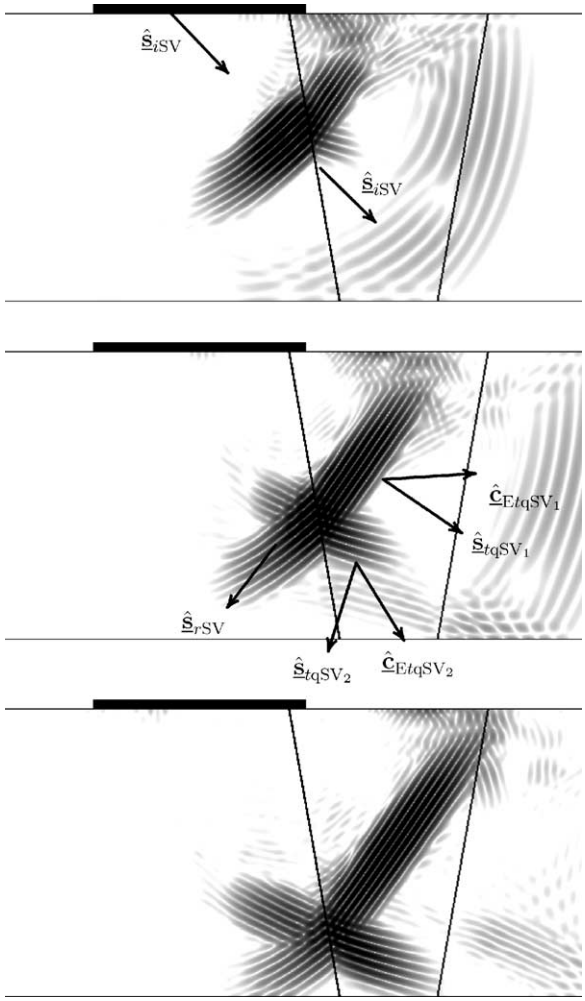

Fig. 7. 2D-EFIT simulation of elastic wave propagation in an austenitic weld: the occurrence of two transmitted qSV-waves is interpreted in terms of transient plane wave energy rays.

It turns out that this result nicely interprets the numerically obtained wave front snap-shots of Fig. 2, as it is overlayed on three selected snap-shots (Fig. 7): A quick estimation on how ultrasonic pulsed rays propagate in an austenitic weld becomes possible.

4. Conclusions

Analytic transient plane wave theory is often helpful to interpret the output of numerical codes for complicated elastic wave propagation environments.

Acknowledgements

The authors thank Dr. U. Mletzko, MPA Stuttgart, for providing the weld micrograph of Fig. 1, Dr. R. Hannemann, former University of Kassel now University of Kentucky, for bringing the weld example to their knowledge and A. Zimmer, University of Kassel, for performing the EFIT simulations of Figs. 2 and 3.

References

[1] A.T. de Hoop, Handbook of Radiation and Scattering of Waves, Academic Press, London, 1995.
[2] M. Spies, Elastic wave propagation in general transversely isotropic media. I. Green's functions and elastodynamic holography, J. Acoust. Soc. Am. 96 (1994) 1144–1157.
[3] P. Fellinger, R. Marklein, K.J. Langenberg, S. Klaholz, Numerical modeling of elastic wave propagation and scattering with EFIT—Elastodynamic Finite Integration Technique, Wave Motion 21 (1995) 47–66.
[4] R. Hannemann, Modeling and imaging of elastodynamic wave fields in inhomogeneous anisotropic media, Dissertation, Universität Kassel, Kassel, 2001. http://www. dissertation.de.
[5] R. Marklein, The Finite Integration Technique as a general tool to compute acoustic, electromagnetic, elastodynamic, and coupled wave fields, in: W.R. Stone (Ed.), Review of Radio Science 1999–2002, IEEE Press/Wiley, Piscataway/New York, 2002, pp. 201–244.
[6] K.J. Langenberg, R. Marklein, K. Mayer, Applications in non-destructive testing, in: P.C. Sabatier, E.R. Pike (Eds.), Scattering, Academic Press, London, 2002, pp. 594–617.
[7] K.J. Langenberg, P. Fellinger, R. Marklein, P. Zanger, K. Mayer, T. Kreutter, Inverse methods and imaging, in: J.D. Achenbach (Ed.), Evaluation of Materials and Structures by Quantitative Ultrasonics, Springer-Verlag, Vienna, 1993, pp. 317–398.
[8] K.J. Langenberg, M. Brandfaß, R. Hannemann, C. Hofmann, T. Kaczorowski, J. Kostka, R. Marklein, K. Mayer, A. Pitsch, Inverse scattering with acoustic, electromagnetic, and elastic waves as applied in nondestructive evaluation, in: A. Wirgin (Ed.), Wavefield Inversion, Springer-Verlag, Vienna, 1999, pp. 59–118.
[9] M. Spies, Elastic waves in homogeneous and layered transversely isotropic media: plane waves and Gaussian wave packets. A general approach, J. Acoust. Soc. Am. 95 (1994) 1748–1760.
[10] H.C. Chen, Theory of Electromagnetic Waves, McGraw-Hill, New York, 1983.
[11] J.D. Achenbach, Wave Propagation in Elastic Solids, North-Holland, Amsterdam, 1973.
[12] B.A. Auld, Acoustic Fields and Waves in Solids, vols. I and II, Wiley, New York, 1973.
[13] D. Royer, E. Dieulesaint, Elastic Waves in Solids, vols. I and II, Springer-Verlag, Berlin, 2000.
[14] R. Marklein, K. Mayer, R. Hannemann, T. Krylow, K. Balasubramanian, K.J. Langenberg, V. Schmitz, Linear and nonlinear inversion algorithms applied in nondestructive evaluation, Inverse Probl. 18 (2002) 1733–1759.
[15] J.P. Wolfe, Imaging Photons: Acoustic Wave Propagation in Solids, Cambridge University Press, Cambridge, 1998.
[16] K. Helbig, Foundations of Anisotropy for Exploration Seismics, Elsevier, Oxford, 1994.
[17] M. Spies, Transducer modeling in general transversely isotropic media via point source synthesis: theory, J. Nondestruct. Eval. 13 (1994) 85–99.